

# Long-term Effects of Red Blood Cell Deposition in an Animal Model of Complicated Atherosclerosis

Stephanie Elaine Gar-Wai Chiu<sup>1</sup>, James Q Zhan<sup>2</sup>, and Alan R Moody<sup>1,2</sup>

<sup>1</sup>Medical Biophysics, University of Toronto, Toronto, Ontario, Canada, <sup>2</sup>Medical Imaging, Sunnybrook Health Sciences Centre, Toronto, Ontario, Canada

**Introduction.** Intraplaque hemorrhage (IPH) may be an important marker of complicated atherosclerotic plaque, due in large part to the proatherosclerotic effects of red blood cells (RBCs) [1]. MRI-detected IPH predicts future ischemic events in both symptomatic [2] and asymptomatic [3] carotid patients. IPH can be simulated by microinfusion catheter delivery of autologous RBCs in a rabbit model of atherosclerosis [4] and the minimally invasive nature of this procedure makes it suited for longitudinal studies of the effects of RBC deposition on advanced plaque evolution. This abstract presents histological and MRI results from 9 weeks after simulated IPH induction.

**Methods.** Advanced plaques were generated in New Zealand White rabbit abdominal aortas ( $n = 8$ ) using a high cholesterol diet and endothelial denudation with an arterial embolectomy balloon catheter. Initiation of the diet was defined as week 0 and denudation was performed at week 1. A 2% cholesterol and 6% peanut oil diet was given until week 1.5, followed by a 0.15% cholesterol and 6% peanut oil diet until sacrifice at week 20. At week 11, rabbits underwent femoral artery catheterization with a microinfusion catheter (modified Bullfrog, Mercator MedSystems, San Leandro, USA) containing a 0.4mm long microneedle. In 4 of the rabbits, 25 $\mu$ l of washed autologous RBCs suspended in 25 $\mu$ l of saline and iodinated contrast agent (Visipaque 320, GE Healthcare Canada, Mississauga, Canada) was injected into 3 discrete sites in the abdominal aorta wall under fluoroscopic guidance. In the other 4 rabbits, RBCs were replaced with saline as a control. Upon sacrifice 9 weeks after injection, the abdominal aorta was excised, formalin-fixed, cut into 5mm blocks, and stained using H&E, Perl's iron stain, anti-CD31 antibody and RAM11 (both antibodies from Dako Canada, Mississauga, Canada). Prior to sacrifice, animals were imaged in a 3.0T Philips Achieva system using the 8-channel head coil. An axial, T1-weighted, 3D turbo field echo sequence was used (0.375mm $\times$ 0.351mm acquired/0.351mm $\times$ 0.351mm reconstructed in-plane, 1.6mm slice thickness, TE/TR/0=5.6ms/16.8ms/15°, turbo factor=60, NEX=3) with ProSet 1-2-1 water excitation and motion-sensitized driven equilibrium T2 preparation (TE=25ms, VENC=5cm/s in all directions). The abdominal aorta was imaged before and after gadofosveset injection (0.2ml/kg, Vasovist, Bayer Schering Pharma, Berlin, Germany).

**Results.** 2 saline control animals died the day after the 2nd catheterization, likely from complications from the microinfusion procedure. H&E sections from these vessels revealed RBC infiltration at injection sites despite only saline and contrast agent being injected. 9 weeks after injection, the only consistent histological indication of RBC or saline injection was a severely disrupted internal elastic lamina. In two of the RBC-injected rabbits, Perl's iron stain revealed iron deposits in neovascularized pockets of foam cells without evidence of concurrent RBC deposition (Fig. 1). In another RBC-injected rabbit, a large clump of intact RBCs was interspersed with foam cells that stained positive for iron (Fig. 2). Two of the RBC-injected rabbits showed iron deposits in the adventitia co-localized with macrophages. Extravasated red blood cells were found within lipid and necrotic cores, with (Fig. 3) and without (Fig. 4) accompanying neovessels. All 6 aortas showed areas of intense intimal neovascularization at multiple sites with these areas accounting for most of the plaque area at times. T1-weighted MR images showed varying vessel wall thickness and post-contrast vessel wall enhancement indicative of the large plaque sizes and extensive inflammation and neovascularization (Fig. 5). **Discussion.** The injection of RBCs results in plaques with features not previously seen in rabbits that underwent similar cholesterol diet and endothelial denudation [4]. Plaques from previous rabbits contained large regions of foam cells with interspersed extracellular cholesterol clefts, but did not feature the acellular necrotic cores observed in this study. The previous plaques also did not demonstrate RBC extravasation, while the plaques in the present study showed extravasated RBCs both in the presence and absence of neovessels. Extravasated RBCs co-localized with CD31-positive neovessels suggest the neovessels a source of RBCs, while the origin of RBCs without accompanying neovessels is unclear. Possible sources for these RBCs could be leakage from the main lumen or previously intact neovessels that have since lost their integrity. It seems unlikely that the large clump of intact RBCs (Fig. 2) came from the main lumen given their deep location. However, if they were from the RBC injection 9 weeks earlier, one would have expected the co-localized macrophages to have broken them down by this time.

It is also unclear as to why only 4 slides had significant intraplaque areas of iron deposition when fluoroscopy confirmed successful delivery in at least one site per rabbit. Adventitial iron deposits suggest a potential route of clearance for RBC-derived iron. Additional studies will need to be conducted with sacrifice closer to the time of RBC injection to monitor the time course of RBC degradation and clearance.

While RBC delivery has been demonstrated in this model, a few refinements are necessary to establish consistency. While fluoroscopy was able to confirm successful vessel wall delivery, not all injection attempts resulted in success. This may be overcome with more careful site selection and injection technique. If the plaque is not thicker than the needle length (0.4mm), then delivery may occur in the adventitia instead. More precise control of needle orientation could maximize chances of intimal and medial delivery. Finally, further work needs to be done to establish a proper non-RBC control since RBCs infiltrated the plaque even in the saline control rabbits.

**Conclusion.** Thick plaques with necrotic cores, large areas of neovascularization and inflammation, extravasated RBCs, and iron deposits result when autologous red blood cells are delivered into advanced plaques. The absence of iron deposits indicated by Perl's iron stain in most slides suggests that most of the RBC-derived iron is cleared from the plaques within 9 weeks of RBC injection. With further refinement of the intraplaque injection technique, an animal model with consistent IPH induction could be established and studied at multiple time points to determine the time course of the degradation and clearance of RBC products as well as their MR signal characteristics.

**References.** [1] Virmani R, Kolodgie FD, Burke AP, et al. *Arterioscler Thromb Vasc Biol.* 2005;25:2054-61. [2] Altaf N, Daniels L, Morgan PS, et al. *J Vasc Surg.* 2008;47:337-42. [3] Singh N, Moody AR, Gladstone DJ, et al. *Radiology.* 2009;252:502-8. [4] Chiu SE, Moody AR, Zhan JQ, Leung G. *Proc of the 19th ISMRM.* 2011.

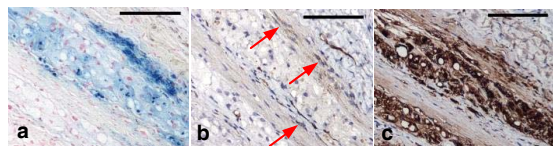


**Fig. 1.** a) Perl's iron stain shows iron deposits (blue) in a collection of foam cells. Both CD31-positive neovessels (b, red arrows) and RAM11 staining (c) co-localize with the deposits.

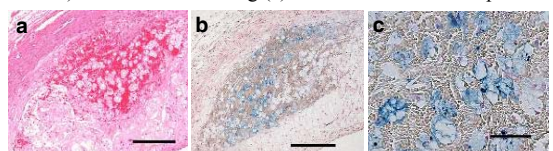


**Fig. 2.** a) H&E stain shows a cluster of RBCs (dark pink) with iron deposits (blue) located within macrophages (b and c).

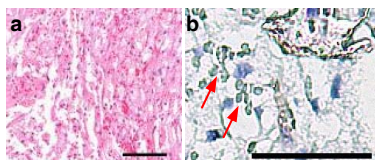


**Fig. 3.** a) H&E stain shows scattered RBCs (dark pink). b) CD31 stain in the same region shows neovessels (brown) and extravasated RBCs (red arrows).

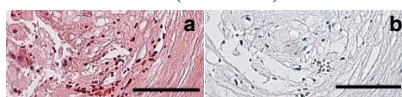


**Fig. 4.** a) H&E stain shows scattered RBCs (red dots). b) CD31 stain in the same region indicates absence of neovessels.

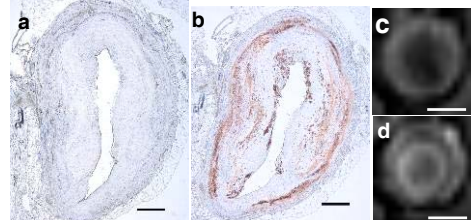


**Fig. 5.** a) CD31 stain shows plaque neovessels covering most of the circumference. b) RAM11 stain shows large regions of inflammation. c) Matching pre-contrast image shows variably thickened wall. d) Post-contrast image shows plaque enhancement.

**Bar** = 50 $\mu$ m in Figs. 2c and 3; 100 $\mu$ m in Figs. 1 and 4; 250 $\mu$ m in Figs. 2a/b; 500 $\mu$ m in Figs. 5a/b; 2mm in Figs. 5c/d.